Identification of C_5H_x Isomers in Fuel-Rich Flames by Photoionization Mass Spectrometry and Electronic Structure Calculations

Nils Hansen,*,† Stephen J. Klippenstein,*,‡ James A. Miller,† Juan Wang,§ Terrill A. Cool,§ Matthew E. Law,⊥ Phillip R. Westmoreland,⊥ Tina Kasper,# and Katharina Kohse-Höinghaus#

Combustion Research Facility, Sandia National Laboratories, Livermore, California 94551, Chemistry Division, Argonne National Laboratory, Argonne, Illinois 60439, School of Applied and Engineering Physics, Cornell University, Ithaca, New York 14853, Department of Chemical Engineering, University of Massachusetts, Amherst, Massachusetts 01003, and Physikalische Chemie I, Universität Bielefeld, D-33501 Bielefeld, Germany

Received: November 30, 2005; In Final Form: January 27, 2006

The isomeric composition of C_5H_x ($x = 2-6$, 8) flame species is analyzed for rich flames fueled by allene, propyne, cyclopentene, or benzene. Different isomers are identified by their known ionization energies and/or by comparison of the observed photoionization efficiencies with theoretical simulations based on calculated ionization energies and Franck−Condon factors. The experiments combine flame-sampling molecular-beam mass spectrometry with photoionization by tunable vacuum-UV synchrotron radiation. The theoretical simulations employ the rovibrational properties obtained with B3LYP/6-311++G(d,p) density functional theory and electronic energies obtained from QCISD(T) electronic structure calculations extrapolated to the complete basis set limit. For C_5H_3, the comparison reveals the presence of both the $H_2CCCCCH$ (*i*-C_5H_3) and the HCCCHCCH (*n*-C_5H_3) isomer. The simulations also suggest a modest amount of *cyclo*-CCHCHCCH−, which is consistent with a minor signal for C_5H_2 that is apparently due to *cyclo*-CCHCCCH−. For C_5H_4, contributions from the CH_2CCCCH_2 (1,2,3,4-pentatetraene), $CH_2CCHCCH$, and CH_3CCCCH (1,3-pentadiyne) isomers are evident, as is some contribution from $CHCCH_2CCH$ (1,4-pentadiyne) in the cyclopentene and benzene flames. Signal at $m/z = 65$ originates mainly from the cyclopentadienyl radical. For C_5H_6, contributions from cyclopentadiene, $CH_3CCCHCH_2$, $CH_3CHCHCCH$, and CH_2CHCH_2CCH are observed. No signal is observed for C_5H_7 species. Cyclopentene, $CH_2CHCHCHCH_3$ (1,3-pentadiene), $CH_3CCCH_2CH_3$ (2-pentyne), and $CH_2CHCH_2CHCH_2$ (1,4-pentadiene) contribute to the signal at $m/z = 68$. Newly derived ionization energies for *i*- and *n*-C_5H_3 (8.20 ± 0.05 and 8.31 ± 0.05 eV, respectively), $CH_2CCHCCH$ (9.22 ± 0.05 eV), and CH_2CHCH_2CCH (9.95 ± 0.05 eV) are within the error bars of the QCISD(T) calculations. The combustion chemistry of the observed C_5H_x intermediates and the impact on flame chemistry models are discussed.

1. Introduction

An improved knowledge of combustion chemistry coupled with the incorporation of this knowledge in kinetic models would provide a valuable aid in the development of more efficient and cleaner combustion processes. The formation of polycyclic aromatic hydrocarbons (PAHs) and ultimately soot remains an especially intriguing problem.[1−4] It now seems clear that fuel structure has a substantial influence on the relative importance of different reactions in the formation of the first aromatic species and higher PAHs. The role of C_5 hydrocarbons in molecular weight growth processes is largely uncertain. The recombination of *cyclo*-C_5H_5 to form naphthalene has been widely accepted, while reactions of *i*-C_5H_3 and C_5H_5 with CH_3 have been postulated as possible routes to benzene formation.[5−7]

Current models for hydrocarbon combustion, which are partially based on species concentration measurements in low-pressure one-dimensional premixed flames, can be greatly improved by taking multiple isomeric forms of all intermediates into account. There are often isomeric forms with quite different chemistries, and therefore, experimental determinations of isomeric compositions are critically needed. To this end a flame-sampling photoionization mass spectrometer for use with bright, easily tunable synchrotron radiation has recently been designed.[8] This new apparatus allows isomer-specific detection of many combustion intermediates. For example, it has been used to identify enols as common intermediates in hydrocarbon combustion.[9]

Combined with high-level electronic structure calculations this extremely powerful new experimental approach has also been used to identify different C_3H_2, C_4H_3, and C_4H_5 isomers.[10,11] Besides the expected cyclopropenylidene, a linear C_3H_2 isomer (propargylene) was detected in a fuel-rich cyclopentene flame.[10] In another paper we showed that *i*-C_4H_3 (CH_2CCCH) and *i*-C_4H_5 (CH_2CHCCH_2) are present in a variety of fuel-rich flames, while the *n*-C_4H_3 (CHCHCCH) and *n*-C_4H_5 ($CHCHCHCH_2$) isomers could not be detected.[11]

In the present work we use flame-sampling photoionization mass spectrometry combined with ab initio electronic structure calculations to identify C_5H_x ($x = 2-6$, 8) isomers in rich flames

* Corresponding authors. Phone: 925-294-6272 (N.H.); 630-252-3596 (S.J.K.). Fax: 925-294-2276 (N.H.); 630-252-9292 (S.J.K.). E-mail: nhansen@sandia.gov (N.H.); sjk@anl.gov (S.J.K.).
† Sandia National Laboratories.
‡ Argonne National Laboratory.
§ Cornell University.
⊥ University of Massachusetts.
Universität Bielefeld.

10.1021/jp0569685 CCC: $33.50
Published on Web 03/07/2006

fueled by allene, propyne, cyclopentene, and benzene. Each mass signal represents contributions from two or more isomers. Identification of different isomers is accomplished by comparing experimental photoionization efficiency (PIE) spectra with simulated curves based on calculated adiabatic ionization energies and Franck−Condon factor analysis. For C_5H_8 we also used measured photoionization efficiency curves of pure cyclopentene and 1,3-pentadiene as guidance.

While the lumped signals for C_5H_x isomers have been mapped in previous work by molecular-beam mass spectrometry (MBMS) with electron ionization, it has not previously been possible to resolve and identify the isomers. Notably, a number of the species detected in this work are not present in current combustion chemistry models. The known chemistry of the various C_5 hydrocarbon isomers, and particularly as it relates to PAH formation, is discussed in detail. Inclusion of all the different observed isomers and their reactions in flame chemistry models should greatly improve their predictive capabilities.

A thorough analysis of those flames considered here, including mole fraction profiles of each species, is beyond the scope of this publication and will be presented in future papers.

2. Experimental Section

The experiment is carried out in a low-pressure premixed flame apparatus at the chemical dynamics beamline at the Advanced Light Source (ALS) at the Lawrence Berkeley National Laboratory. The technique of molecular-beam time-of-flight photoionization mass spectrometry is fully described elsewhere.[8] In general, photoionization has become a major technique for research in the physical sciences. Single-photon ionization usually occurs in the vacuum-UV region and is the most general and cleanest photoionization method.[12,13]

The experiment consists of a low-pressure flame chamber, a differentially pumped flame-sampling system, and a time-of-flight mass spectrometer (TOFMS). Flame gases are sampled through the 0.20 mm orifice of a quartz sampling cone on the flow axis of a flat-flame burner operated at typical pressures of 30 torr. Translation of the burner toward or away from the quartz sampling cone allows mass spectra to be taken at any desired position within the flame. A skimmer of 2.0 mm aperture placed 23 mm downstream on the axis of the expanded (10^{-4} torr) jet forms a molecular beam that passes into the differentially pumped (10^{-6} torr) ionization region, where it is crossed by tunable vacuum-UV light. The resulting photoions are separated by using pulsed-extraction time-of-flight mass spectrometry and detected with a multichannel plate (MCP). A multiscaler records TOF mass spectra in 15 008 channels of 2 ns width.

The flame apparatus uses tunable undulator radiation, energy-selected by a 3 m off-plane Eagle monochromator. A rare gas filter removes contributions from higher undulator harmonics, and an energy resolution of either 25 or 40 meV full width at half-maximum (fwhm), measured from the observed width of autoionizing resonances in O_2,[14,15] is employed. The photon flux passing through the ionization region is measured with a silicon photodiode calibrated at the National Institute of Standards and Technology (NIST) for quantum efficiency (electron/photon) in the energy range from 8 to 15 eV.

In the present experiments, allene, propyne, cyclopentene, and benzene were used as fuels. Fuel-rich allene and propyne flames are of particular interest as both molecules are potential precursors for C_3H_3 radicals, thus enhancing the importance of the propargyl recombination process to form benzene.[16] Cyclopentene flames are of interest because the cyclopentadienyl radical, a possible precursor of benzene and naphthalene,[5,6] is present in large concentrations. Benzene flames are interesting for at least two reasons. Benzene is the simplest aromatic hydrocarbon and is thus the prototype for aromatic combustion, and since aromatics make up a substantial fraction of most real fuels the oxidation of benzene is of fundamental interest. Furthermore, although the rate-limiting step in PAH and soot formation is believed to be the formation of benzene, most of the molecular weight growth process happens after benzene formation. Thus, by starting with benzene, we can look at the chemistry leading to higher molecular weight species.

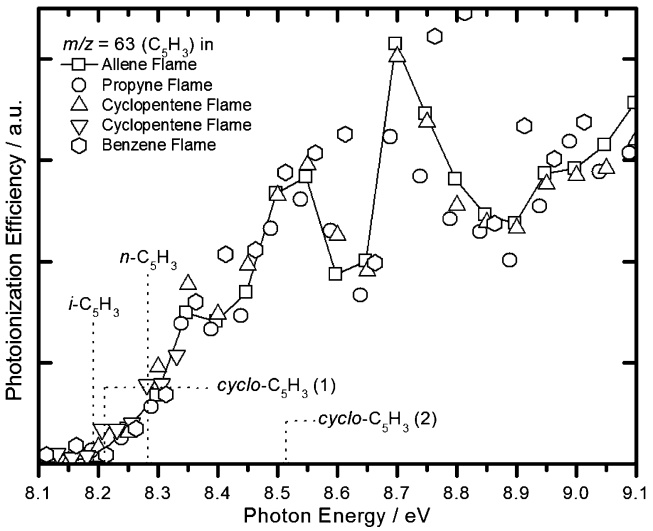

Figure 1. Measured photoionization efficiency curves for $m/z = 63$ (C_5H_3) in fuel-rich allene, propyne, cyclopentene, and benzene flames. The second set of cyclopentene flame data (▽) was recorded with a 0.025 eV step-width, rather than a 0.05 eV step-width. In addition, calculated ionization energies of four different isomers are marked.

Allene and propyne flames have not been studied before; for the cyclopentene and benzene flames, different conditions from the limited number of previous studies[17−19] are chosen, sufficiently below the sooting limit to avoid deposition on the sampling probe. The following conditions are used:

- allene or propyne/oxygen/40.8% argon flames with a fuel/oxygen equivalence ratio ϕ (fuel/oxygen ratio relative to a stoichiometric mixture) = 1.80 at a pressure of 25.0 torr and a cold-flow reagent velocity of 48.2 cm/s;
- cyclopentene/oxygen/25% argon flame with an fuel/oxygen equivalence ratio $\phi = 2.00$ at a pressure of 37.6 torr and a cold-flow reagent velocity of 54.7 cm/s;
- benzene/oxygen/38.5% argon flame with a fuel/oxygen equivalence ratio $\phi = 1.66$ at a pressure of 35.0 torr and a cold-flow reagent velocity of 29.2 cm/s.

To determine photoionization efficiencies (PIE), the ion signals at a given m/z ratio are obtained by integration of the accumulated ion counts per channel over a 60 ns time interval centered about the mass peak, from which the baseline contribution, obtained from the signal between peaks, is subtracted. This approach permits integration over the entire temporal profile of each mass peak, while avoiding overlapping contributions from adjacent mass peaks. The baseline-corrected ion signals are corrected for the contributions of ^{13}C and ^{2}H isotopomers and finally are normalized by the photon flux.

Observed PIE spectra are shown in Figures 1−5 for the C_5H_x ($x = 3-6$, 8) species from each of the flames. The data are taken at 3.5 and 3.25 mm distance from the burner for the allene (propyne) and cyclopentene flames, respectively. At the chosen positions, a simultaneous measurement of the PIE curves of most C_5 species is possible. For the benzene flame, $m/z = 63$ and 64

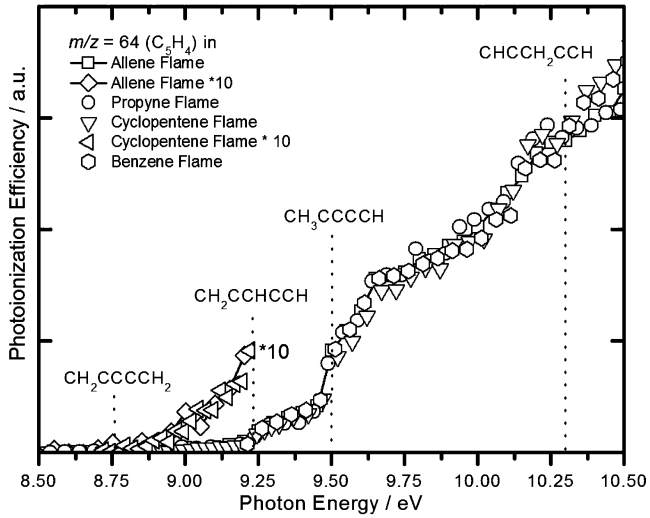

Figure 2. Observed photoionization efficiency curves for $m/z = 64$ (C_5H_4) in fuel-rich allene, propyne, cyclopentene, and benzene flames. The region between 8.5 and 9.25 eV is shown enlarged for the allene and cyclopentene flames. In addition, the known and/or calculated ionization energies of four different isomers are marked.

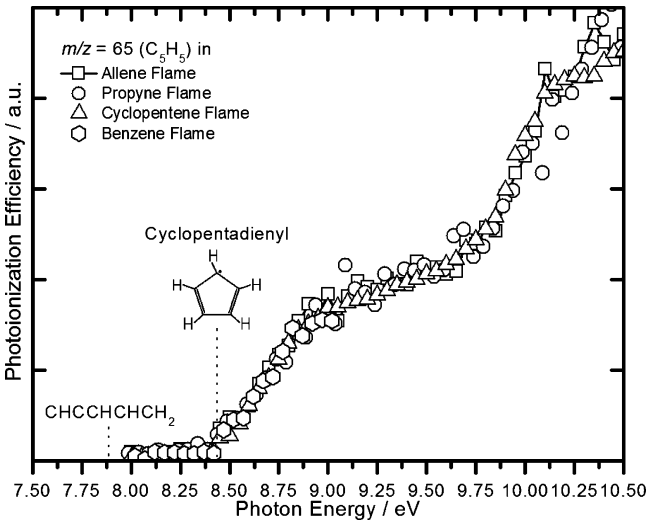

Figure 3. Observed photoionization efficiency curves for $m/z = 65$ (C_5H_5). The ionization energy of the most stable *cyclo*-C_5H_5 (cyclopentadienyl) radical at 8.41 eV is marked as is the ionization energy of the linear $CHCCHCHCH_2$ radical at 7.88 eV. The signal is dominated by the cyclopentadienyl radical although some small signal below its threshold of 8.41 eV is detected. The ionization energies of the linear isomers are beyond the photon energy range.

data are taken at 4.5 mm distance from the burner, while $m/z = 65$ and 66 PIE curves are measured at 5.5 mm. Although the number densities of the species differ in each flame, the PIEs of Figures 1−5 have been vertically scaled for ease of comparison. The observed PIE curves for different flames look nearly identical, and therefore the isomeric composition of the flames is qualitatively similar, while there still might be quantitative differences.

In principle, it is possible to determine absolute mole fractions of every single isomer in each flame. However, often the electronic transition moments for the photoionization of single isomers are not known, and therefore analysis based on Franck−Condon factors does not immediately yield an estimate of the relative concentration of all different isomers. A direct determination of isomeric composition will require knowledge of the respective cross sections for photoionization of each isomer. Reasonable estimations for absolute photoionization cross

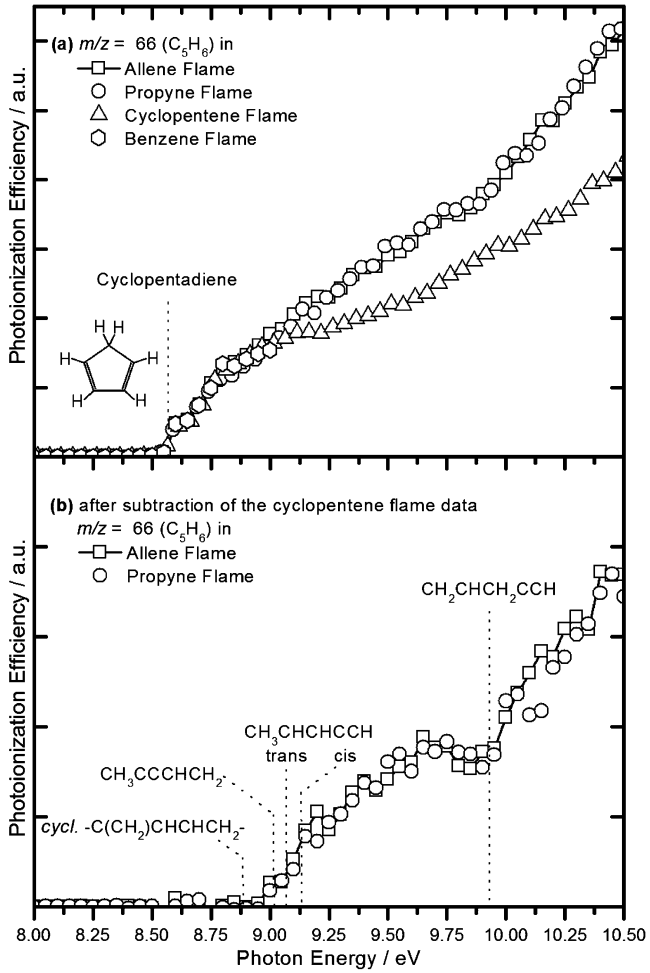

Figure 4. (a) Measured photoionization efficiency curves for $m/z = 66$ (C_5H_6) in the energy range from 8.0 to 10.5 eV in fuel-rich allene, propyne, cyclopentene, and benzene flames. We note that the signal, especially in the cyclopentene flame, is dominated by the contribution of 1,3-cyclopentadiene. The subtraction of the $m/z = 66$ signal in the cyclopentene flame from the signal in the allene and propyne flame yields the signal which is shown in (b). See text for details. In addition, the calculated and/or known ionization energies of likely isomers are indicated.

sections can be made on the basis of known cross sections for molecules with similar functional groups. Such estimates should yield absolute concentrations that are accurate to within about a factor of 2.

3. Computational Methodology

The geometries and rovibrational properties of various neutral and cationic isomers of C_5H_x ($x = 2-6$, 8) are obtained with density functional theory employing the Becke-3 Lee−Yang−Parr (B3LYP) hybrid functional[20] and the 6-311++G(d,p) basis set.[21] These density functional evaluations, which are performed with Gaussian03 quantum chemical software,[22] employ unrestricted spin wave functions for all open-shell species and spin-restricted wave functions for all singlets. The geometrical structures, harmonic vibrational frequencies, and rotational constants for each of the species are provided in the Supporting Information. For C_5H_4, C_5H_6, and C_5H_8 the neutral isomers are generally presumed to be singlets and the cations are generally presumed to be doublet radicals. For C_5H_3 and C_5H_5 the neutral isomers are generally presumed to be doublet radicals, while for the cations both singlet and triplet species are considered. For C_5H_2 both singlet and triplet states are considered for the

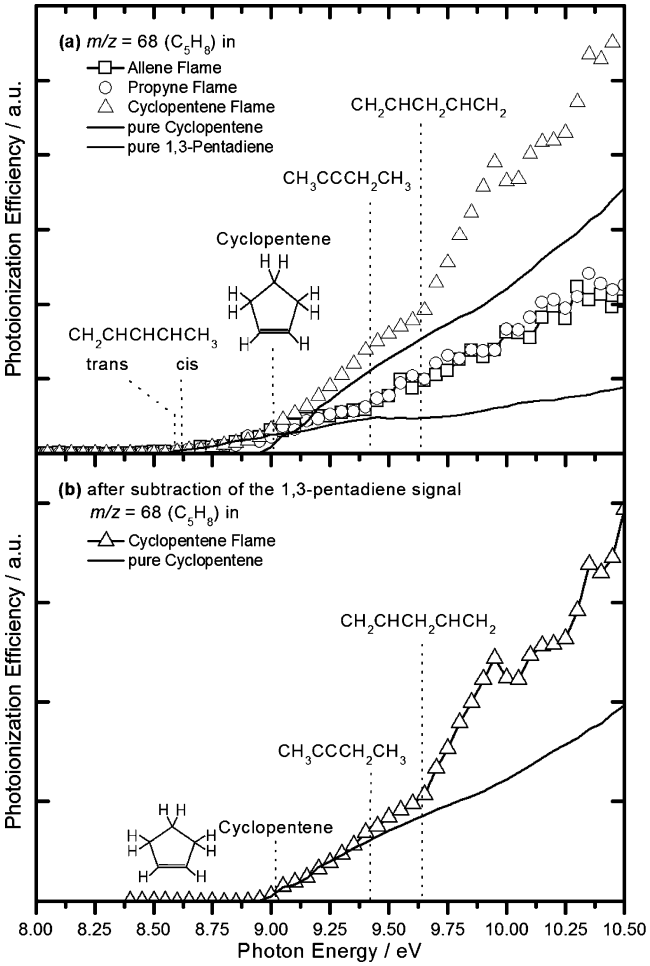

Figure 5. (a) Observed photoionization efficiency curves for $m/z = 68$ (C_5H_8) in fuel-rich allene, propyne, cyclopentene, and benzene flames. The calculated and/or known ionization energies of several C_5H_8 isomers are indicated. In addition, measured photoionization efficiency curves for pure *trans*-1,3-pentadiene and cyclopentene are shown as solid lines. (b) The residual photoionization efficiency curve of $m/z = 68$ (C_5H_8) in the cyclopentene flame after subtraction of the *trans*-1,3-pentadiene contribution.

neutral species, while doublet states are considered for the cations unless the ground state of the neutral is a triplet, in which case a quartet state is also considered. The symmetry of the electronic states considered is generally taken to be that chosen by the SCF procedure in Gaussian03. However, for CH_3CCCC and related species, both σ and π radical states are considered.

Higher-level energies, E_{HL}, for the various species are obtained from the basis set extrapolation of quadratic configuration interaction calculations (QCISD(T)) employing Dunning's correlation-consistent triple- and quadruple-ζ basis sets,[23] as described in ref 10. These higher-level evaluations are performed with the MOLPRO[24] quantum chemistry software and include the B3LYP/6-311++G(d,p) harmonic zero-point energy corrections. With this level of theory one expects the predicted heats of formation and ionization energies to be accurate to within ~1 or 2 kcal/mol. For some of the larger open-shell species with C_1 optimal geometries, the higher-level energies are instead obtained for related higher-symmetry geometries (i.e., in C_s symmetry) and an estimate of the geometry relaxation energy is obtained from smaller basis set QCISD(T) calculations. For the C_5H_8 species the predictions of ionization energies employ the extrapolation scheme of ref 16, which replaces the QCISD(T) quadruple-ζ evaluations with MP2 ones. For each of the species the Q1 diagnostic of Lee et al. is evaluated.[25] A value of greater than 0.02 for Q1 indicates the presence of significant multireference character to the wave function, with the uncertainties in the energy estimates increasing as Q1 increases beyond 0.02. Heats of formation are calculated by considering H_2 and CH_4 as reference species; i.e., the heats of formation are obtained via the consideration of decomposition reactions producing CH_4, using H_2 as a chemical balance and the experimental heats of formation for H_2 and CH_4.

TABLE 1: Heats of Formation of Different C_5H_2 isomers

species	$\Delta_f H^0$ (0 K) (kcal mol^{-1}) QCISD(T)	Q1 diag[a]
cyclo-C(CCH)CCH−	174.0	0.014
^{3}CHCCCCH	175.0	0.025
CH_2CCCC	187.7	0.022
cyclo-CCHCCCH−	216.1	0.031
cyclo-CCCHCHC−	223.8	0.047

[a] Q1 diagnostic parameter according to Lee et al. (25). Q1 > 0.02 indicates significant multireference character to the wave function.

The simulations of photoionization efficiency spectra based on Franck−Condon factors employ the force-constant matrixes, unscaled frequencies, and normal mode displacements calculated at the B3LYP/6-311++G(d,p) level for the ground states of the neutral and cationic isomers considered here. No contributions from excited states of the ions are taken into account. The evaluation of overlap integrals is carried out in the harmonic approximation, accounting for Duschinsky rotation. Multidimensional overlap integrals are evaluated according to recursion relations.[26,27] The calculations are carried out using a program developed by Winter, Zwier, and Lehmann.[28] The resulting Franck−Condon factors, including hot bands arising from thermal population at the assumed temperature, are integrated and convolved with a Gaussian response function corresponding to the measured experimental photon energy resolution of 40 meV (fwhm).

4. Results and Discussion

In this paper, different C_5H_x ($x = 2-6$, 8) isomers in fuel-rich flames are identified by their ionization energies, by comparison of observed photoionization efficiency curves with simulated curves based on Franck−Condon factor analysis, or by comparison with measured photoionization efficiency curves of pure substances. This part of the paper is organized as follows: In the first section, we summarize the calculated thermodynamic properties of several species considered in this paper. Then, the experimental photoionization efficiency curves are compared with simulations based on a Franck−Condon factor analysis. Finally, the impact on flame chemistry models is discussed.

4.1. Calculated Thermodynamic Properties. *C_5H_2.* For completeness, different C_5H_2 isomers are included, although experimental evidence in the form of a weak signal is only found in the cyclopentene flame. Calculated heats of formation for five different C_5H_2 isomers are summarized in Table 1. According to the present electronic structure calculations, the most stable C_5H_2 isomer is the three-membered *cyclo*-C(CCH)-CCH−, while the linear ^{3}CHCCCCH and CH_2CCCC species are less stable by 1 and 14 kcal/mol, respectively. Related prior CCSD(T)/cc-pvtz calculations instead suggest that the ^{3}CHC-CCCH species is the most stable (by 2 kcal/mol) and that CH_2-CCCC is 13.8 kcal/mol above that.[29] The heats of formation for two five-membered ring isomers are predicted to be 216.1 kcal/mol (*cyclo*-CCHCCCH−) and 223.8 kcal/mol (*cyclo*-CCCHCHC−).

TABLE 2: Ionization Energies of Different C_5H_2 Isomers

species	ion state	ionization energies/eV calculated	Q1 diag
cyclo-C(CCH)CCH−	$^2A'$	8.90	0.025
^{3}CHCCCCH	$^2\Pi_u$	8.39	0.027
CH_2CCCC	$^2B_2$	9.48	0.038
cyclo-CCHCCCH−	^2B	8.51	0.026
cyclo-CCCHCHC−	$^2A''$	8.85	0.035

TABLE 3: Heats of Formation of Different C_5H_3 Isomers

species	Δ_fH^0 (0 K) (kcal mol^{-1}) QCISD(T)	literature[a]	Q1 diag
i-C_5H_3	137.2	136.2	0.023
n-C_5H_3	138.8	137.0	0.019
cyclo-C(CCH)CHCH−	168.0	167.8	0.016
cyclo-CCHCHCCH−	171.8	169.6	0.017
CH_3CCCC (π)	178.0		0.025
CH_3CCCC (σ)	182.9		0.014
cyclo-CHCCCHCH−	179.9	179.4	0.051

[a] G2M(rcc,MP2) values from ref 30 converted to 0 K values using B3LYP/6-311++G** harmonic vibrational frequencies.

TABLE 4: Ionization Energies of Different C_5H_3 Isomers

species	ion state	ionization energies/eV calculated	measured	Q1 diag
i-C_5H_3	$^1A_1$	8.19	8.20 ± 0.05	0.024
n-C_5H_3	$^1A_1$	8.28	8.31 ± 0.05	0.021
cyclo-C(CCH)CHCH−	$^1A_1$	6.19		0.014
cyclo-CCHCHCCH−	$^1A'$	8.21		0.015
CH_3CCCC	$^3A_1$	9.50		0.025
cyclo-CHCCCHCH−	$^1A'$	8.50		0.043

Calculated ionization energies, ranging between 8.4 and 9.5 eV, for these C_5H_2 isomers are shown in Table 2. Signal at $m/z = 62$ is detected above an apparent ionization threshold of 8.5 eV, suggesting the presence of the five-membered *cyclo*-CCHCCCH−. However, the signal is quite weak, and hence, contributions from other isomers can not be ruled out.

C_5H_3. Energies of 25 different isomers of C_5H_3 have been calculated earlier by Mebel et al.,[30] who found that the linear $H_2CCCCCH$ (*i*-C_5H_3) and HCCCHCCH (*n*-C_5H_3) forms are the most stable ones with heats of formation (0 K) of 136.2 and 137.0 kcal/mol, respectively.

The results of our QCISD(T) calculations of 137.2 and 138.8 kcal/mol for *i*-C_5H_3 and *n*-C_5H_3, respectively, agree well with these values. In addition, heats of formation of several other isomers are calculated, including the linear CH_3CCCC, the *cyclo*-C(CCH)CHCH−, and the two most stable five-membered rings, *cyclo*-CCHCHCCH− [*cyclo*-C_5H_3 (1)] and *cyclo*-CHCCCHCH− [*cyclo*-C_5H_3 (2)]. These data are summarized in Table 3.

Calculated adiabatic ionization energies for several C_5H_3 isomers are summarized in Table 4. As can be seen in Figure 1, the ionization energies of 8.19 and 8.28 eV for the *i*-C_5H_3 and *n*-C_5H_3 isomers, respectively, are both close to the observed ionization threshold. For the next most stable linear isomer, CH_3-CCCC, which lies 31 kcal/mol above the most stable form (cf., Table 3), we calculate an ionization energy of 9.50 eV. The resonantly stabilized *cyclo*-C(CCH)CHCH−, lying 30 kcal/mol above the ground state, has a calculated ionization energy of 6.19 eV. Because no signal is observed below 8.2 eV, a contribution from this isomer is ruled out. We also considered the presence of the two most stable five-membered rings. The calculated ionization energies for *cyclo*-CCHCHCCH− and *cyclo*-CHCCCHCH− are 8.21 and 8.50 eV.

TABLE 5: Heats of Formation of Different C_5H_4 Isomers

species	Δ_fH^0 (0 K) (kcal mol^{-1}) QCISD(T)	literature	Q1 diag
CH_3CCCCH	100.5	101.1[a]	0.013
$CH_2CCHCCH$	106.0		0.014
CH_2CCCCH_2	108.7	111.1[a]	0.016
$CHCCH_2CCH$	110.2		0.013
cyclopentadienylidene (T)	125.8	127.4,[b] 127.5[c]	0.018
(S)	131.5	133.6[b]	0.028

[a] CCSD(T)/cc-pvtz values from ref 31. [b] Averge of G2(MP2,SVP) and G2(B3LYP/MP2,SVP) values from ref 33. [c] G2M(RCC,MP2) from ref 61 converted to 0 K using B3LYP/6-311++G** harmonic frequencies.

C_5H_4. A variety of different C_5H_4 isomers might be expected to play roles in combustion processes, the most obvious one being CH_3CCCCH (1,3-pentadiyne). Other linear C_5H_4 isomers such as $CH_2CCHCCH$, CH_2CCCCH_2 (1,2,3,4-pentatetraene), and $CHCCH_2CCH$ (1,4-pentadiyne) may also be significant in flames. Calculated heats of formation (0 K) for these isomers are presented in Table 5 together with the heat of formation of the *cyclo*-CCHCHCHCH− (cyclopentadienylidene radical). As can be seen in Table 5, 1,3-pentadiyne is the most stable C_5H_4 isomer. Its calculated heat of formation of 100.5 kcal/mol agrees well with the previously calculated value of 101.1 kcal/mol from Woodcock et al.[31] The $CH_2CCHCCH$ is predicted to be 6 kcal/mol less stable. The 1,4-pentadiyne isomer is calculated to be less stable than 1,3-pentadiyne by about 10 and 2 kcal/mol less stable than the cumulene-type structure, 1,2,3,4-pentatetraene. Cyclopentadienylidene is higher in energy than 1,3-pentadiyne by about 25 kcal/mol.

The calculated ionization energies of the C_5H_4 isomers are summarized in Table 6. By comparison with available literature values we conclude that our calculations agree with previous experimental data to within 0.1 eV. The observed threshold near 8.7 eV is most likely due to the CH_2CCCCH_2 (1,2,3,4-pentatetraene) isomer, although at this point a contribution from the cyclic five-membered ring cyclopentadienylidene (calculated ionization energy = 8.67 eV) cannot be ruled out. The increase in photoionization efficiency near 9.25 eV is most likely due to the presence of the $CH_2CCHCCH$ isomer. The calculated ionization energy of 9.24 eV fits the observation as shown in Figure 2. The calculated value of 9.47 eV (C_s symmetry) for the most stable C_5H_4 isomer, 1,3-pentadiyne, fits the observed sharp rise near 9.5 eV. The relatively high ionization threshold of 10.3 eV for 1,4-pentadiyne may make it difficult to detect above the background from the other isomers. Furthermore, since it is less stable than the other linear isomers, it is unlikely to be present in high concentrations.

C_5H_5. The most stable C_5H_5 isomer is the *cyclo*-C_5H_5 radical (cyclopentadienyl) which is known to be a common combustion intermediate in rich flames and a potential precursor for benzene and naphthalene.[5−7] In addition, several linear C_5H_5 isomers are conceivable. The calculated heats of formation are summarized in Table 7 and compared with literature data. A large number of other isomers were considered by Moskaleva et al.,[7] but these isomers are all significantly less stable and so are unlikely to be relevant. The most stable linear isomer is the resonantly stabilized $CHCCHCHCH_2$, which is less stable than cyclopentadienyl by 30 kcal/mol. Two other five-membered rings, *cyclo*-$CH_2CHCHCCH$− and *cyclo*-$CH_2CHCHCHC$−, are calculated to be higher in energy than the cyclopentadienyl isomer by 34 kcal/mol. Heats of formation for three additional linear isomers are calculated to be between 109.9 and 115.6

TABLE 6: Ionization Energies of Different C_5H_4 Isomers

species	ion state	ionization energies/eV calculated	measured	literature	Q1 diag
CH_3CCCCH	$^2A''$	9.47	9.50 ± 0.05	9.51 ± 0.02[a,b]	0.025
$CH_2CCHCCH$	$^2A''$	9.24	9.22 ± 0.05		0.028
CH_2CCCCH_2	$^2B_3$	8.76	8.76 ± 0.05	8.67 ± 0.02[b,c]	0.023
$CHCCH_2CCH$	$^2B_1$	10.32	10.28 ± 0.08	10.27 ± 0.02[b]	0.016
cyclopentadienylidene	$^4B_2$	(T) 8.67 (S) 8.42			0.016

[a] Ref 40. [b] Ref 36. [c] Ref 62.

TABLE 7: Heats of Formation of Different C_5H_5 Isomers

species	Δ_fH^0 (0 K) (kcal mol^{-1}) QCISD(T)	literature	Q1 diag
cyclo-CHCHCHCHCH−	65.5	65.4 ± 1.0,[a] 65.9 ± 1.0[b] 67.1,[c] 66.3,[c] 69.9[d]	0.014
$CHCCHCHCH_2$ (trans)	95.3	99.5,[d] 90.8[e]	0.019
(cis)	95.6		0.019
$CH_2CHCCCH_2$	98.4		0.022
cyclo-$CH_2CHCHCCH$−	98.5		0.014
cyclo-$CH_2CHCHCHC$−	99.1	104.0[d]	0.014
CH_2CCCCH_3	109.9		0.014
$CH_3CHCCCH$	113.3		0.013
$CH_2CCHCCH_2$	115.6		0.018

[a] Experimental value from ref 63. [b] Experimental value from ref 64 converted to 0 K using B3LYP/6-311++G** harmonic vibrational frequencies. [c] G2(MP2) values from ref 65. [d] G2M(RCC,MP2) values from ref 58. [e] Experimental value from ref 43 converted to 0 K using B3LYP/6-311++G** harmonic vibrational frequencies.

TABLE 8: Ionization Energies of Different C_5H_5 Isomers

species	ion state	ionization energies/eV calculated	measured	literature	Q1 diag
cyclo-CHCHCHCHCH−	$^3B_2$	8.40	8.40 ± 0.05	8.41[a]	0.010
	$^1A_1$	8.66			0.017
$CHCCHCHCH_2$ (trans)	$^1A'$	7.82		7.88[b]	0.018
(cis)	$^1A'$	7.89			0.019
$CH_2CHCCCH_2$	$^1A'$	7.74			0.022
cyclo-$CH_2CHCHCCH$−	$^3A''$	8.17			0.015
cyclo-$CH_2CHCHCHC$−	$^3A''$	8.63			0.024
cyclo-$CH_2CHCHCHC$−	$^1A'$	8.34			0.025
CH_2CCCCH_3	$^1A'$	7.37			0.021
$CH_3CHCCCH$	$^1A'$	7.73			0.023
$CH_2CCHCCH_2$	$^1A'$	7.09			0.019

[a] Ref 32. [b] Ref 43.

kcal/mol and, therefore, about 45 kcal/mol less stable than cyclopentadienyl.

The calculated ionization energies for all the C_5H_5 isomers considered here are provided in Table 8. The calculated ionization energy of 8.40 eV for *cyclo*-C_5H_5 (cyclopentadienyl) agrees well with the literature value of 8.41 eV[32] and fits the observed PIE curve, which is in shown in Figure 3. Obviously, the signal is dominated by the cyclopentadienyl radical, although some weak signal is seen below its ionization threshold. This signal is most likely due to the presence of a linear isomer, although we were not able to measure the ionization threshold, which is below 8 eV.

C_5H_6. The C_5H_6 isomer most likely to be present in significant amounts in fuel-rich flames is certainly 1,3-cyclopentadiene. The heat of formation (0 K) of 1,3-cyclopentadiene is calculated to 35.8 kcal/mol at the QCISD(T) level of theory, which is in agreement with previous literature values.[33−35] In addition, the heats of formation for another 13 isomers are calculated and are summarized in Table 9. By far the most stable isomer is 1,3-cyclopentadiene, with all linear structures being higher in energy by at least 28 kcal/mol. The second most stable ring structure is the four-membered *cyclo*-$C(CH_2)CHCHCH_2$− (methylene-cyclobutene), which is actually the third most stable C_5H_6 isomer overall. The heats of formation for five different three-membered rings are also calculated to be between 80 and

TABLE 9: Heats of Formation of Different C_5H_6 Isomers

species	Δ_fH^0 (0 K) (kcal mol^{-1}) QCISD(T)	literature	Q1 diag
1,3-cyclopentadiene	35.8	35.7[a], 37.0[a] 36.2[b] 36.9,[c] 36.1,[c] 39.2[c]	0.011
$CH_3CCCHCH_2$	62.2		0.012
cyclo-$C(CH_2)CHCHCH_2$−	63.3		0.012
$CH_3CHCHCCH$ (cis)	63.7	65.0[a]	0.012
(trans)	64.1	65.2[a]	0.012
$CH_3C(CH_2)CCH$	64.0	65.2[a]	0.012
$CH_2CHCHCCH_2$ (trans)	64.0		0.013
(cis)	66.4		0.012
CH_2CHCH_2CCH	68.8		0.012
$CH_3CHCCCH_2$	72.5		0.014
cyclo-$C(CH_2)CH_2C(CH_2)$−	80.8		0.012
cyclo-$C(CCH_2)CH_2CH_2$−	82.7		0.012
cyclo-$C(CH_3)CHC(CH_2)$−	84.3		0.013
cyclo-$C(CHCH_3)CHCH$−	90.2		0.012
cyclo-$C(CH_3)CHCHCH$−	95.4		0.013
cyclo-$CH_2CH_2CH_2CC$−	115.3		0.014

[a] Experimental values from ref 34 converted to 0 K using B3LYP/6-311++G** harmonic vibrational frequencies. [b] G2(MP2,SVP) value from ref 33. [c] G2 values from ref 35 with different bond additivity corrections.

84 kcal/mol which is about 50 kcal/mol higher than the 1,3-cyclopentadiene. The heat of formation of a cyclopentyne

TABLE 10: Ionization Energies of Different C_5H_6 Isomers

species	ion state	ionization energies/eV calculated	measured	literature	Q1 diag
1,3-cyclopentadiene	$^2A_2$	8.58	8.57 ± 0.05	8.57 ± 0.01[a]	0.013
$CH_3CCCHCH_2$	$^2A'$	9.01	9.00 ± 0.05	9.00 ± 0.01[b]	0.015
cyclo-$C(CH_2)CHCHCH_2-$	$^2A''$	8.89			0.030
$CH_3CHCHCCH$ (cis)	$^2A''$	9.11	9.11 ± 0.05	9.11 ± 0.01[b]	0.020
(trans)	$^2A''$	9.10	9.05 ± 0.05	9.05 ± 0.01[b]	0.018
$CH_3C(CH_2)CCH$	$^2A''$	9.25		9.25 ± 0.02[b,c]	0.023
$CH_2CHCHCCH_2$ (trans)	$^2A''$	8.78		8.88 ± 0.02[c]	0.027
(cis)	$^2A''$	8.76			0.025
CH_2CHCH_2CCH	$^2A''$	9.87	9.95 ± 0.05		0.032
$CH_3CHCCCH_2$	^2A	8.72			0.027

[a] Ref 44. [b] Ref 45. [c] Ref 36.

TABLE 11: Heats of Formation of Different C_5H_8 Isomers

species	Δ_fH^0 (0 K) (kcal mol^{-1}) QCISD(T)	literature[a]	Q1 diag
cyclopentene	13.7	14.0[b]	0.010
$CH_2CHC(CH_2)CH_3$	23.2	23.5 ± 0.2[c]	0.011
$CH_2CHCHCHCH_3$ (trans)	23.5	23.3 ± 0.2[c]	0.011
(cis)	24.8	25.0 ± 0.2[c]	0.011
$CH_2CHCH_2CHCH_2$ (gauche)	30.0	30.7 ± 0.3[c]	0.011
(cis)	30.2		0.011
cyclo-$C(CH_3)CHCH_2CH_2-$	33.3		0.010
cyclo-$C(CH_2)CH_2CH_2CH_2-$	34.4	34.9 ± 0.2,[d] 31.2[d]	0.010
$CH_3CCCH_2CH_3$	35.0	35.6 ± 0.5[c]	0.011
$CH_2CC(CH_3)_2$	35.3	35.9 ± 0.1[d]	0.011
$CH_3CHCCHCH_3$	36.7	36.8 ± 0.2[c]	0.011
$CHCCH(CH_3)_2$	38.0	37.6 ± 0.5[d]	0.010
$CH_3CH_2CHCCH_2$ (gauche)	38.4	38.6 ± 0.2[c]	0.011
(cis)	38.3		0.011
$CH_3CH_2CH_2CCH$ (trans)	39.2	39.5 ± 0.5[d]	0.011
(gauche)	39.2		0.010

[a] The 298 K values from the literature have been converted to 0 K using the B3LYP/6-311++G** harmonic vibrational frequencies. [b] Experimental values from ref 66. [c] Experimental values from ref 67. [d] Experimental values from ref 34.

structure (*cyclo*-$CH_2CH_2CH_2CC-$) is calculated to be 115.3 kcal/mol. With such high heats of formation these last six ring species are unlikely to be present in flames.

The calculated ionization energies are summarized in Table 10 and compared with literature values, when available. In general, the agreement between our calculations and the literature values is remarkable. The only exception is for the $CH_2CHCHCCH_2$ isomer, where theory predicts an ionization energy of 8.79 eV, while the experimentally observed value is 8.88 ± 0.02 eV. Comparison of the calculated values with the PIE curves in Figure 4a suggests that the observed threshold near 8.6 eV reflects the presence of 1,3-cyclopentadiene in those flames. Contributions from other isomers are difficult to identify. Figure 4b illustrates the residual photoionization efficiency curves in the allene and propyne flames, obtained by subtracting the $m/z = 66$ signal in the cyclopentene flame. The details of this residual PIE curve are discussed together with the Franck−Condon simulations in section 4.2.

C_5H_7. The signal at $m/z = 67$ appears to be entirely caused by ^{13}C isotopomers of $m/z = 66$. Therefore, C_5H_7 isomers are considered to be present at levels near or beneath the threshold of detection and are not further considered in this paper.

C_5H_8. A number of C_5H_8 isomers may play a role in combustion chemistry. Calculated heats of formation and ionization energies for the most likely C_5H_8 isomers are summarized in Tables 11 and 12.

Cyclopentene is the most stable C_5H_8 isomer and a known combustion intermediate. Its calculated heat of formation (0 K) of 13.7 kcal/mol is lower by at least 10 kcal/mol than those of all other isomers. For example, the heat of formation of the 1,3-pentadiene ($CH_2CHCHCHCH_3$) isomer is calculated to be 23.5 kcal/mol. Again, some four-membered rings are considered: the calculated heats of formation for the *cyclo*-$C(CH_3)CHCH_2CH_2-$ and *cyclo*-$C(CH_2)CH_2CH_2CH_2-$ isomers are 33.3 and 34.4 kcal/mol, respectively, which makes them 20 kcal/mol higher in energy than the cyclopentene isomer. The calculated heats of formation are in good agreement with the experimental data.

Calculated ionization energies are in the range of 8.6 to 10.0 eV. The lowest ionization energy calculated for the different C_5H_8 isomers is that for 1,3-pentadiene at 8.65 eV (Table 12), which matches the observed threshold as shown in Figure 5a. As will be discussed in section 4.2, Figure 5a compares observed photoionization efficiency curves in the allene (propyne) and cyclopentene flames with PIE curves of pure 1,3-pentadiene and cyclopentene. Figure 5b compares the residual PIE curve in the cyclopentene flame after subtraction of the 1,3-pentadiene contribution. A sharp increase in photoionization efficiency can be observed near 9.0 eV, the ionization threshold of cyclopentene.

A remarkable consistency is observed between calculated ionization energies and known literature values. The only two exceptions are the $CH_3CHCCHCH_3$ and the $CH_3CH_2CHCCH_2$ isomers. Both these species contain C═C═C moieties. The transition from the neutral species to the ion causes a significant torsional rotation about these C═C═C bonds. However, if we constrain the symmetry of the ion to be C_S (like the neutral ground state), our calculations yield an IE of 9.26 eV for the $CH_3CH_2CHCCH_2$ isomer, which is in good agreement with the experimental value of 9.25 eV.[36]

4.2. Identification of the Isomers and Franck−Condon Modeling of the Photoionization Efficiency Spectra. Throughout this paper the isomers are identified in different ways. Whenever possible we compare observed photoionization efficiency curves with calculated and/or known ionization energies and known photoionization efficiency curves of pure substances. However, isomers were identified for the most part by comparing observed photoionization efficiency spectra with simulated photoionization efficiency curves based on Franck−Condon factor analysis. The photoionization efficiency spectra of different C_5 isomers are simulated using a calculated Franck−Condon envelope as a fitting function to estimate the adiabatic ionization energies of those isomers from the experimental data. A similar strategy was previously employed to derive the ionization energies of C_3H_2 (triplet propargylene),[10] C_4H_3 and C_4H_5 radicals,[11] and HONO[37] from flame measurements. The simulations presented here are for an assumed temperature of 300 K. The temperatures in the sampled regions of the flames

TABLE 12: Ionization Energies of Different C_5H_8 Isomers

species	ion state	ionization energies/eV calculated	measured	literature	Q1 diag
cyclopentene	$^2A'$	9.04	9.00 ± 0.05	9.01 ± 0.01[a]	0.022
$CH_2CHC(CH_2)CH_3$	$^2A''$	8.90		8.85 ± 0.02[a]	0.025
$CH_2CHCHCHCH_3$ (trans)	$^2A''$	8.63	8.60 ± 0.05	8.59 ± 0.02[b]	0.024
(cis)	$^2A''$	8.65		8.62 ± 0.03[b]	0.020
$CH_2CHCH_2CHCH_2$ (gauche)	^2A	9.17		9.62 ± 0.02[a]	0.013
(cis)	^2A	9.60			0.013
cyclo-$C(CH_3)CHCH_2CH_2-$	^2A	8.94			0.016
cyclo-$C(CH_2)CH_2CH_2CH_2-$	$^2A'$	9.16		9.19 ± 0.02[a]	0.018
$CH_3CCCH_2CH_3$	$^2A''$	9.44		9.44 ± 0.02[a]	0.019
$CH_2CC(CH_3)_2$	^2B	8.86		8.95 ± 0.02[a]	0.020
$CH_3CHCCHCH_3$	^2A	8.88		9.13 ± 0.02[a]	0.025
$CHCCH(CH_3)_2$	^2A	10.00		10.05 ± 0.02[a]	0.024
$CH_3CH_2CHCCH_2$ (gauche)	^2A	8.84		9.25 ± 0.02[a]	0.021
(cis)	^2A	8.83			0.020
$CH_3CH_2CH_2CCH$ (trans)	^2A	10.04		10.10 ± 0.02[a]	0.028
(gauche)	^2A	10.04			0.028

[a] Ref 36. [b] Ref 46.

are considerably higher than 300 K, but significant cooling occurs in the expansion through the sampling nozzle. Rotational temperatures of NO sampled from similar flames have been measured to be between 300 and 400 K with little sensitivity to the initial sampling temperature.[38] In addition, photoionization efficiency curves of stable species, sampled at similar flame temperatures, agree well with room-temperature measurements.[39]

C_5H_3. The observed photoionization efficiency of C_5H_3 (Figure 1) can be well fit between 8.1 and 8.4 eV by a weighted sum of the 300 K Franck−Condon simulations for the two most stable C_5H_3 isomers. The fit is shown in Figure 6a. The simulation for *i*-C_5H_3 ($H_2CCCCCH$) presented as a dotted line is based on an adiabatic ionization energy of 8.20 eV. The simulation shows small contributions from hot bands below the adiabatic ionization energy of 8.20 eV, a stepped increase near the threshold, and a nearly constant photoionization efficiency above the ionization energy.

The calculated spectrum for *i*-C_5H_3 closely resembles the observed PIE curve below 8.3 eV but fails to explain the second step visible in the experimental PIE curve at this energy. This step arises from a contribution of the *n*-C_5H_3 isomer (HCCCH-CCH), which is shown as a dashed line. In this simulation the ionization energy of *n*-C_5H_3 is fixed at 8.31 eV. The simulated photoionization efficiency curve is similar to the one for the *i*-C_5H_3 isomer. Contributions from hot bands are visible below the assumed ionization energy of 8.31 eV; a stepped increase near the threshold resembles the step in the observed PIE curve, and for energies above 8.31 eV, the calculated photoionization efficiency stays nearly constant. For both isomers, the uncertainty in the adiabatic ionization energies is estimated to be ±0.05 eV, and therefore the ionization energies of *n*-C_5H_3 and *i*-C_5H_3 are reported as 8.20 ± 0.05 and 8.31 ± 0.05 eV, respectively. Assuming equal absolute photoionization cross sections for both the *i*- and the *n*-C_5H_3 isomers at 8.6 eV, the best simulation is for an *n*-C_5H_3/*i*-C_5H_3 ratio of about 3:1.

An even better fit can be obtained when a contribution is included from the *cyclo*-CCHCHCCH− form, the most stable five-membered ring. Its simulated photoionization efficiency spectrum is shown as a short-dashed line in Figure 6b. The inclusion of such a contribution may explain the observed slow increase in photoionization efficiency between 8.4 and 9.1 eV. Again assuming equal absolute photoionization cross sections for all three isomers at 8.6 eV, the best simulation is for a *n*-C_5H_3/*i*-C_5H_3/*cyclo*-CCHCHCCH− ratio of 9:3:1.

The possible presence of the *cyclo*-CCHCHCCH− isomer is consistent with a (weak) signal observed at $m/z = 62$ (C_5H_2)

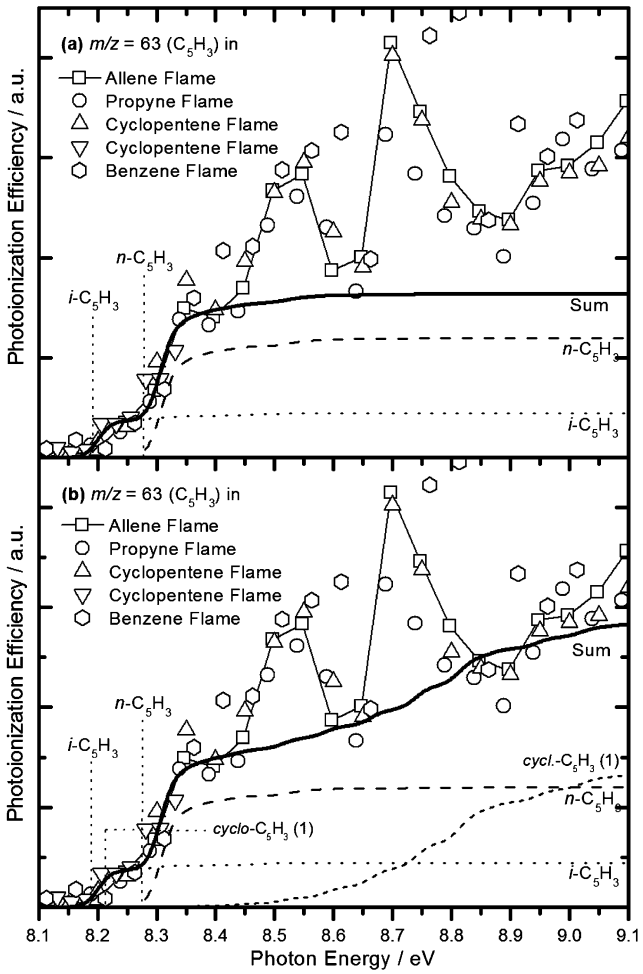

Figure 6. (a) Comparison of the observed photoionization efficiency curves for C_5H_3 as shown in Figure 1 with a simulation based on a Franck−Condon factor analysis. Contributions from both of the most stable isomers, *n*- (dashed) and *i*-C_5H_3 (dotted), are clearly visible. (b) A better fit, explaining the slowly rising photoionization efficiency curve in the region from 8.4 to 9.1 eV, can be achieved by taking into account contributions from the *cyclo*-CCHCHCCH− isomer (short-dashed).

with an apparent threshold of 8.5 eV. Our calculations (Table 2) suggest the presence of *cyclo*-CCHCCCH− which can easily be formed by H abstraction from *cyclo*-CCHCHCCH−.

The Franck−Condon simulation for the *cyclo*-CHCCCHCH− isomer, which is not shown, exhibits a sharp rise near the

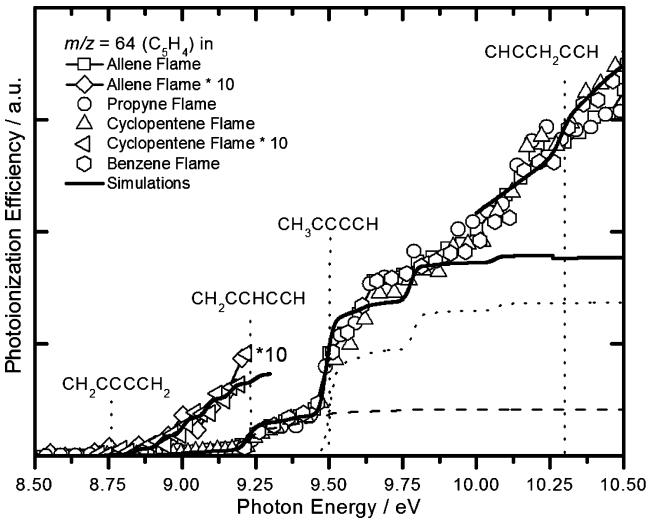

Figure 7. Comparison of the observed photoionization efficiency curves for C_5H_4 as shown in Figure 2 with Franck−Condon-factor-based simulations. The region between 8.5 and 9.25 eV can be nicely fit by contributions from the CH_2CCCCH_2 isomer. Two other isomers, $CH_2CCHCCH$ and CH_3CCCCH, can be clearly identified. Some contribution from the $CHCCH_2CCH$ isomer may be visible above its ionization energy of 10.3 eV.

calculated ionization energy of 8.5 eV and is not helpful in interpreting the observed photoionization efficiency. The full simulation does not account for the broad peaks seen at 8.5 and 8.7 eV, which are probably poorly resolved autoionization resonances.

C_5H_4. The observed photoionization efficiency of C_5H_4 (Figure 2) can be well fit between 8.75 and 10.0 eV by a weighted sum of the 300 K Franck−Condon simulations for the three most stable C_5H_4 isomers. The fit is shown in Figure 7. The region near the observed threshold at 8.7 eV can be nicely reproduced by contributions from the cumulene-type CH_2CCCCH_2 isomer, assuming an adiabatic ionization energy of 8.76 eV. The simulation shows a slow increase in photoionization efficiency between 8.75 and 9.25 eV.

However, the calculated spectrum for CH_2CCCCH_2 alone fails to explain the first sharp step visible in the experimental PIE curve at 9.25 eV. This step may be fit by a contribution from the $CH_2CCHCCH$ isomer, which is shown as a dashed line. For this contribution the adiabatic ionization energy is fixed at 9.22 eV, a value in near perfect agreement with the present QCISD(T) theoretical predictions (Table 6). The simulated photoionization efficiency curve shows a stepped increase near the threshold that resembles the step in the observed PIE curve. For energies above 9.25 eV, the calculated photoionization efficiency slowly increases, including a small step near 9.5 eV.

The sharp increase in photoionization efficiency which is observed near 9.5 eV for all of the flames is certainly due to the presence of the most stable CH_3CCCCH (1,3-pentadiyne) isomer. For the simulated PIE curve shown as a dotted line in Figure 7 an ionization energy of 9.50 eV was assumed, a value identical with literature and calculated values.[40] The simulation, which shows a sharp step in photoionization efficiency near 9.5 eV and a smaller step near 9.75 eV, is limited by not taking into account Jahn−Teller splitting for the ground state of the cation. Nonetheless qualitative agreement between theory and experiment is achieved between 9.5 and 10.0 eV. Again, absolute photoionization cross sections for all isomers are not known, but, using estimated values, a ratio for CH_2CCCCH_2/$CH_2CCHCCH$/CH_3CCCCH of approximately 1:5:20 is determined.[41] This ratio is expected to depend on distance from the burner, reflecting differing chemistries of these isomers.

For all three isomers, the uncertainties in the adiabatic ionization energies are estimated to be ±0.05 eV, and therefore the ionization energies of CH_2CCCCH_2, $CH_2CCHCCH$, and CH_3CCCCH are reported as 8.76 ± 0.05, 9.22 ± 0.05, and 9.50 ± 0.05 eV, respectively.

The presence or absence of the $CHCCH_2CCH$ isomer (1,4-pentadiyne) in the flames studied in this paper is difficult to ascertain. Careful comparisons of the photoionization efficiencies obtained for allene and propyne flames with those obtained for cyclopentene and benzene flames reveal small differences near 10.3 eV. A small increase in photoionization efficiency is observed in the latter flames. The observed "threshold" of these differences matches the literature value (10.27 ± 0.02 eV)[36] and calculated ionization energy (10.32 eV) for $CHCCH_2CCH$. The full simulation shown in Figure 7 for the 10.0−10.5 eV range includes a contribution from this isomer based on an ionization energy of 10.28 eV. The simulation in this range also assumes a "background" linear increase with photon energy from the other isomers. The simulated curve fits the experimental data quite nicely, with the improved agreement suggestive of the presence of 1,4-pentadiyne in the cyclopentene and benzene flames.

C_5H_5. As can be seen in Figure 3, the observed photoionization efficiency curves in the fuel-rich allene, propyne, cyclopentene, and benzene flames look qualitatively the same. Several isomers exist, but it is reasonable to assume that the $m/z = 65$ signal in the cyclopentene flame is largely due to the presence of the cyclopentadienyl radical (*cyclo*-C_5H_5). Therefore, the photoionization efficiency curve in the fuel-rich cyclopentene flame is a particularly good estimate for the shape of the PIE curve of the cyclopentadienyl radical. The *cyclo*-C_5H_5 (cyclopentadienyl) radical is then clearly identified in all four flames both by the shape of the observed PIE curves and by the observed ionization energy near the literature value of 8.41 eV.[32] The increase in photoionization efficiency above 9.6 eV is probably due to excited states of the ion. Some additional signal, resulting from a linear C_5H_5 isomer, is observed. Experimental limitations did not allow the determination of such a low ionization energy, but in a similar experiment by Qi et al., at the University of Science at Technology of China (USTC) in Hefei, China,[42] an ionization energy near 7.8 eV was determined, most likely due to either the resonantly stabilized $CHCCHCHCH_2$ or the $CH_2CHCCCH_2$ isomer.[43]

C_5H_6. The identification of different C_5H_6 isomers is largely based on the Franck−Condon factor analysis. Figure 4a shows that the observed threshold near 8.6 eV is due to the presence of the most stable isomer, 1,3-cyclopentadiene, with an ionization energy of 8.57 eV.[44] We infer that the $m/z = 66$ signal in the cyclopentene flame is largely dominated by 1,3-cyclopentadiene. The $m/z = 66$ signals between 8.6 and 9.0 eV are then normalized, and the reference signal from the cyclopentene flame is subtracted from the signals in the allene and propyne flames. This subtraction results in the residual photoionization efficiency curves shown in Figure 4b. Another threshold is clearly visible near 9.0 eV.

The Franck−Condon factor simulation for 1,3-cyclopentadiene isomer nicely reproduces the observed photoionization efficiency curve for cyclopentadiene in the 8.5−9.0 eV region, as illustrated in Figure 8. For the simulations an ionization energy of 8.57 eV was assumed, which is identical with literature[44] and the present quantum chemical calculations as summarized in Table 10.

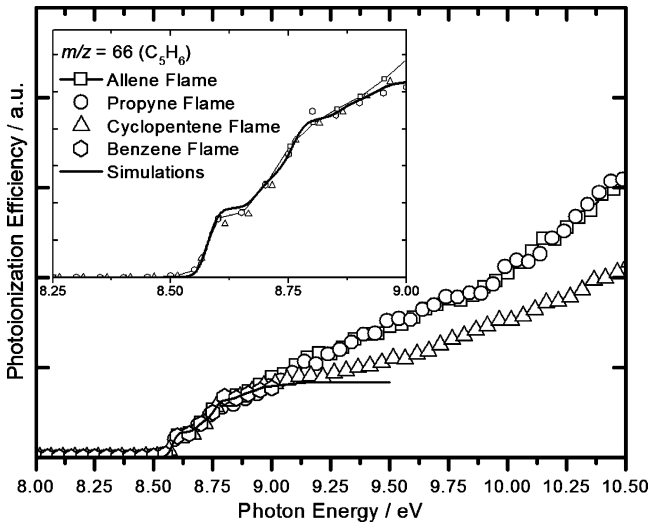

Figure 8. Comparison of the observed photoionization efficiency curves for $m/z = 66$ (C_5H_6) in fuel-rich flames with Franck−Condon-factor-based simulations for the cyclopentadiene isomer. An excellent match between the observed data and the calculations is achieved for photon energies in the range from 8.5 to 9.0 eV.

Figure 9 summarizes our attempts to fit the residual photoionization efficiency curve shown in Figure 4b. The simulation for the $CH_3CCCHCH_2$ isomer shown in Figure 9a is based on an ionization energy of 9.00 eV.[45] The simulated photoionization efficiency curve reproduces the observed threshold near 9.0 eV, but in general it fails to explain the characteristics of the observed PIE curve. Figure 9b shows a comparison of the observed residual PIE curve with a Franck−Condon-factor-based simulation for the $CH_3CHCHCCH$ isomer. The simulation is based on ionization energies of 9.05 and 9.11 eV for the trans and cis isomers, respectively, and assumes a Boltzmann distribution of these isomers at an elevated flame temperature of 2000 K. Both values agree with known values from the literature[45] and the present quantum chemical calculations (Table 10). The simulation for this species, Figure 9b, provides a greatly improved reproduction of the observed residual photoionization efficiency curve between 9.1 and 10.0 eV. However, we notice that the simulation fails to explain the small ion signal near 9.0 eV. Last, but not least, Figure 9c shows the Franck−Condon factor simulation for the *cyclo*-$C(CH_2)CHCHCH_2$− isomer based on the calculated ionization energy of 8.89 eV. The shape of the calculated photoionization efficiency curve looks similar to the one shown in Figure 9b, but the calculated ionization energy does not match our observations. Therefore, in accord with expectations, we can rule out the existence of the four-membered *cyclo*-$C(CH_2)CHCHCH_2$− species in any of the flames.

In summary, besides the most stable 1,3-cyclopentadiene,we have clearly identified the presence of the $CH_3CCCHCH_2$ and the *cis*/*trans*-$CH_3CHCHCCH$ isomers. Figure 10 summarizes the overall fit of the simulated PIE curves to the observed residual PIE curve. The fit is based on contributions from the $CH_3CCCHCH_2$ isomer (dashed), from a mixture of *cis*- and *trans*-$CH_3CHCHCCH$ isomers (dotted), and from the CH_2-$CHCH_2CCH$ isomer (short-dashed). The latter contribution helps to reproduce the observed increase near 10.0 eV. The simulation for CH_2CHCH_2CCH is based on an ionization energy of 9.95 eV, a value slightly larger than the calculated value of 9.88 eV. No evidence was found for the branched $CH_3C(CH_2)CCH$, the CH_2CHCH_2CCH isomer, or the $CH_3CHCCCH_2$ isomers. With the use of the estimated absolute photoionization cross sections, the 1,3-cyclopentadiene/*cis*/*trans*-$CH_3CHCHCCH$/CH_2-$CHCH_2CCH$/$CH_3CCCHCH_2$ ratio was determined to be 8:3:2.5:1. Again, this ratio may vary with burner position if the different isomers undergo differing chemistries.

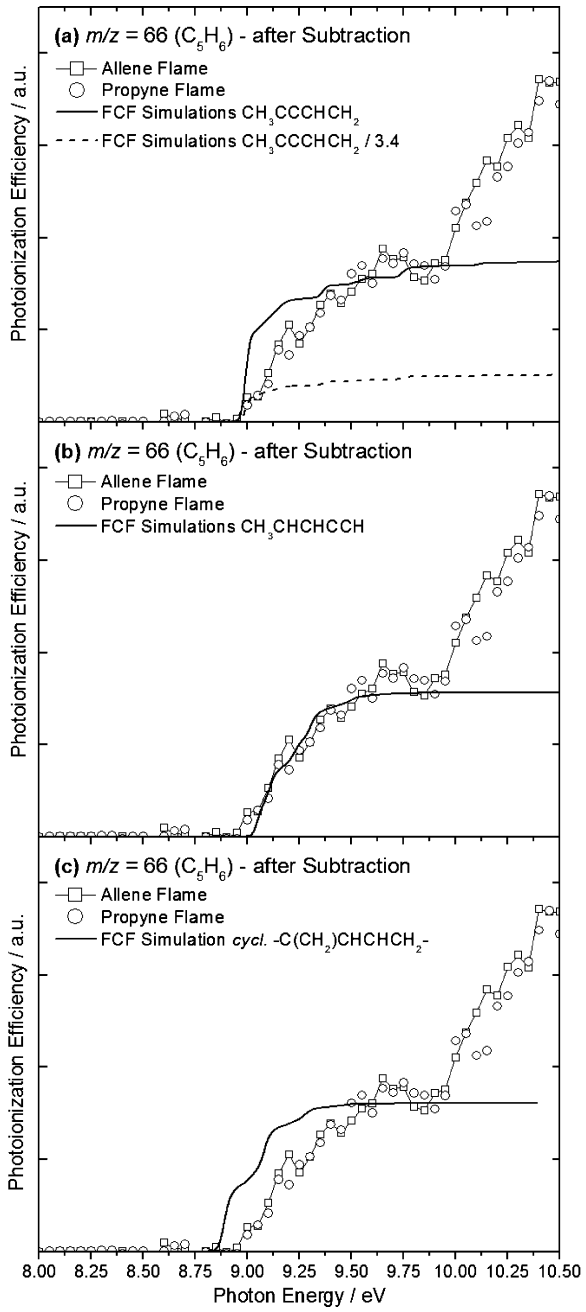

Figure 9. (a) Comparison of the residual photoionization efficiency signal as shown in Figure 4b with Franck−Condon-factor-based simulations for the $CH_3CCCHCH_2$ isomer. The simulation shows that it can explain the threshold near 9.0 eV but fails to explain the shape of the curve for photon energies larger than 9.1 eV. (b) Comparison of the residual photoionization efficiency signal with simulations for a mixture of the *cis*/*trans*-$CH_3CHCHCCH$ isomers. The simulations fail to match the low-energy region near 9.0 eV but fit the data nicely up to 9.9 eV. (c) Comparison of the residual photoionization efficiency signal with a simulation for the *cyclo*-$C(CH_2)CHCHCH_2$− isomer. The fit fails to match the observed photoionization efficiency curves.

C_5H_8. Different C_5H_8 isomers in fuel-rich allene, propyne, and cyclopentene flames were identified by their ionization energies and by comparison of the observed photoionization efficiency curves with measured PIE curves of pure, standard substances. No Franck−Condon-factor-based simulations were needed. As can be seen in Figure 5a, the observed threshold in the photoionization efficiency curves is near 8.6 eV, a value

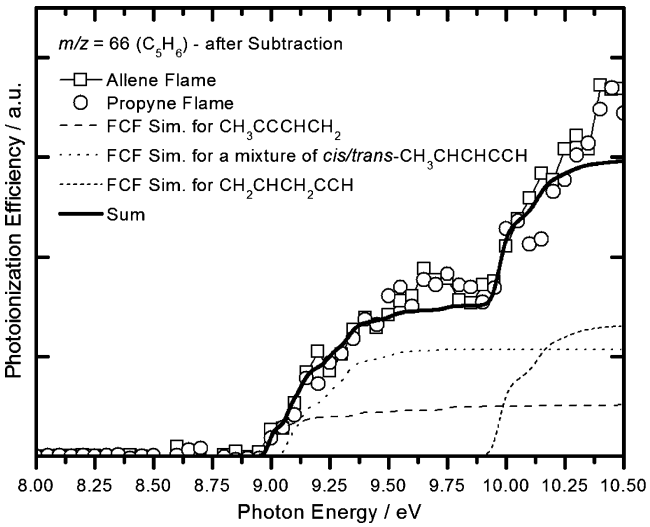

Figure 10. Overall fit of the residual photoionization efficiency curve for $m/z = 66$ with calculations based on a Franck−Condon factor analysis. Contributions from $CH_3CCCHCH_2$, a mixture of *cis*/*trans*-$CH_3CHCHCCH$, and CH_2CHCH_2CCH are considered.

close to the known threshold of *cis*/*trans*-$CH_2CHCHCHCH_3$ (1,3-pentadiene), the two different isomers having nearly equal ionization energies.[46] Figure 5a shows the photoionization efficiency curve of pure *trans*-1,3-pentadiene, and it is assumed that *cis*-1,3-pentadiene shows a qualitatively similar photoionization efficiency. The observed curve for the pure substance is identical with the observed curve in the flames from 8.6 throughout 9.0 eV. An increase in photoionization efficiency is observed near 9.0 eV, which is absent in the PIE curve of 1,3-pentadiene. However, cyclopentene should be observed above its threshold of 9.01 eV.[36] As a reference the PIE curve of pure cyclopentene is shown in Figure 5, parts a and b, as a solid line.

Because the photoionization efficiency of 1,3-pentadiene was measured, we subtracted that signal from the measured PIE curves of $m/z = 68$ in the fuel-rich cyclopentene flame. The resulting residual PIE curve is shown in Figure 5b with a definite threshold near 9.0 eV, in perfect agreement with the known ionization energy of cyclopentene. A comparison of this residual PIE curve with that of pure cyclopentene indicates the presence of $CH_3CCCH_2CH_3$ (2-pentyne) and $CH_2CHCH_2CHCH_2$ (1,4-pentadiene). Using the known absolute photoionization cross sections [1,3-pentadiene, 6.6 Mb (9.0 eV), 18.8 Mb (10.25 eV); cyclopentene, 11.6 Mb (10.25 eV) − 1 Mb (megabarn) = 10^{-18} cm^2],[47] we calculated the 1,3-pentadiene/cyclopentene ratio. For the allene/propyne flame, a 1:1 ratio was determined, while in the cyclopentene flame a ratio of 1:4 is determined. For the cyclopentene flame we determine the cyclopentene/1-pentyne/1,4-pentadiene ratio at the chosen burner position to 12:1:4.

4.3. Combustion Chemistry. *C_5H_3.* In its first measurement by MBMS with electron ionization, $m/z = 63$ appeared with an ionization threshold of 9.1 eV in the fuel-rich benzene flame of Bittner ($\phi = 1.8$).[18] He speculated that it might be the H_2-CCCCCH radical (*i*-C_5H_3), analogous to propargyl (C_3H_3), but the present results show that species to have an ionization energy of 8.20 eV. Delfau and Vovelle[48] and Westmoreland and coworkers[49,50] measured C_5H_3 profiles in fuel-rich C_2H_2 flames. In the latter work, an ionization threshold was measured as 8.4 ± 0.25 eV. This low resolution does not allow identification of C_5H_3 isomers such as was achieved here.

The C_5H_3 isomers (*i*-C_5H_3 and *n*-C_5H_3) share some important properties with propargyl: they are both resonantly stabilized, they both have strong C−H bonds, and *i*-C_5H_3 can be formed by the reaction of singlet or triplet methylene with diacetylene (reaction paths to *n*-C_5H_3 are less obvious). The latter reactions are analogous to the ones forming propargyl from acetylene. The strong C−H bonds are a consequence of lying at the end of a sequence of linear species, starting with C_5H_{12} in this case and C_3H_8 in the case of propargyl, for which removing the weakest bound hydrogen atom results either in a stable molecule or a radical with a weak C−H bond. The last species in such sequences are radicals that must either dissociate into a triplet radical or a carbene, both of which are less stable than an ordinary molecule. Based on electronic structure calculations of Mebel et al.,[30] Pope and Miller suggested that *i*-C_5H_3 could react with CH_3 to form benzene, fulvene, or phenyl + H,[5] but the "energy window" for such a reaction proves to be only about 7 kcal/mol (i.e., the highest rearrangement barrier lies only 7 kcal/mol below the entrance channel, whereas for $C_3H_3 + C_3H_3$ the analogous window is ∼30 kcal/mol[3,16,51,52]), suggesting that the reaction may be very slow. Preliminary calculations of the rate coefficient indicate that this is, in fact, the case, but it is possible that a more energetically favorable path may ultimately be found, restoring interest in this reaction.

C_5H_5. By far the most important of the C_5 species is the cyclopentadienyl radical, *cyclo*-C_5H_5. This species was first detected in the fuel-rich benzene flame of Bittner.[18,53] In most current combustion models *cyclo*-C_5H_5 is formed primarily from phenyl, C_6H_5, through the sequence,[3]

$$C_6H_5 + O_2 \rightarrow C_6H_5O + O \qquad \text{(R1)}$$

or

$$C_6H_5 + OH \rightarrow C_6H_5O + H \qquad \text{(R2)}$$

followed by the dissociation of phenoxy,

$$C_6H_5O \rightarrow \textit{cyclo}\text{-}C_5H_5 + CO \qquad \text{(R3)}$$

The reaction of cyclopentadienyl with itself then becomes a primary source of naphthalene in rich flames through the sequence proposed by Melius et al.,[6]

$$\textit{cyclo}\text{-}C_5H_5 + \textit{cyclo}\text{-}C_5H_5 \rightarrow C_5H_5C_5H_4 + H \qquad \text{(R4a)}$$

$$C_5H_5C_5H_4 \rightarrow C_{10}H_8 + H \qquad \text{(R4b)}$$

where $C_{10}H_8$ is naphthalene.

As a consequence, cyclopentadienyl is believed to be an important intermediate in the growth of higher hydrocarbons, PAH, and soot in rich flames. Because it is also formed from thermal decomposition of benzyl radical,[54] it should also be important in pyrolysis. Accurate measurements of its concentrations in low-pressure flame experiments should go a long way in helping to clarify its role. Quantitative cyclopentadienyl burner profiles have already been reported in different flames. For example, it has been shown that the reaction of *cyclo*-C_5H_5 with CH_3 might be a relevant benzene formation pathway[7] and that reactions R4a and R4b are a main production channel for naphthalene formation.[17,55,56]

Other C_5 Isomers. Other C_5 species play lesser roles in the growth of higher hydrocarbons in combustion, at least according to current conventional wisdom. In fact, many of the species detected in the present experiments do not even appear in combustion models. However, signals from such species have long been observed. C_5H_6 was first observed in 1965 by Homann and Wagner,[57] and Delfau and Vovelle[48] and Westmoreland and

co-workers[49,50] measured profiles for the species from C_5H_2 through C_5H_6.

1,3-Cyclopentadiene is thought to be formed in most flames from *cyclo*-C_5H_5, either by combining with or abstracting a hydrogen atom, but we can only speculate about how other C_5 species detected in our experiments might arise. For example, CH_3CCCCH is a possible product of the chemically activated addition reaction,

$$C_4H_2 + CH_3 \rightarrow CH_3CCCCH + H \qquad (R5)$$

This reaction is roughly 10 kcal/mol endothermic, but it could come into play at high temperatures. The reaction of propargyl with acetylene forms *cyclo*-C_5H_5 at low temperatures,[58,59]

$$C_3H_3 + C_2H_2 \rightarrow \textit{cyclo}\text{-}C_5H_5 \qquad (R6)$$

However, at conditions typical of the high-temperature reaction zones of premixed flames, the equilibrium of reaction (R6) shifts to favor the dissociation of cyclopentadienyl into propargyl plus acetylene. The question of whether other products could be formed at high temperature from $C_3H_3 + C_2H_2$ naturally arises, since C_3H_3 and C_2H_2 are generally present in rich flames in fairly large quantities. Fragmentation of the initial adducts in this reaction could produce either $CH_2CCHCCH + H$ or $CHCCH_2CCH + H$. However, both of these sets of products are substantially endothermic (on the order of 20 kcal/mol), and only a detailed, quantitative analysis can say whether such reactions could be the source of these species in our flames. The formation of the *cyclo*-C_5H_4 isomers (+ H) from $C_3H_3 + C_2H_2$ appears to be prohibitively endothermic.

5. Conclusions

In the present work, several isomers of C_5H_x ($x = 2-6$, 8) have been identified in fuel-rich allene, propyne, cyclopentene, and benzene flames. Distinction between isomers was made possible by combining flame-sampling photoionization mass spectrometry with high-level ab initio electronic structure calculations. A wealth of information for chemical kinetic modeling is provided, and we hope that such models can be made more accurate and robust by considering our results.

In detail, a comparison of the measured photoionization efficiency for C_5H_3 with a Franck−Condon simulation, based on ab initio calculations of frequencies and force constants, reveals the presence of the linear *i*-C_5H_3 ($H_2CCCCCH$) and *n*-(HCCCHCCH) isomers. Other identified species at $m/z = 64$ include CH_2CCCCH_2, $CH_2CCHCCH$, CH_3CCCCH, and probably $CHCCH_2CCH$. Besides the *cyclo*-C_5H_5 isomer (cyclopentadienyl radial), signal from a linear isomer is also seen. At $m/z = 66$ up to five different isomers could be identified. Besides the most stable 1,3-cyclopentadiene, $CH_3CCCHCH_2$ was clearly identified, as were CH_2CHCH_2CCH and $CH_3CHCHCCH$. Signals at $m/z = 68$ (C_5H_8) were composed of at least four different isomers. The most stable species (cyclopentene), CH_2-$CHCHCHCH_3$ (1,3-pentadiene), $CH_3CCCH_2CH_3$ (2-pentyne), and $CH_2CHCH_2CHCH_2$ (1,4-pentadiene) are present in fuel-rich flames.

Absolute mole fraction profiles can be derived according to a recipe described earlier by Cool et al.[60] Concentration profiles of individual isomers are obtained by precise tuning of the photon energies to minimize interferences caused by ionization of multiple species of the same or nearly equal masses. Determination of absolute concentrations requires the knowledge of absolute photoionization cross sections. However, a detailed discussion of mole fraction profiles and their derivation for these different intermediates in different flames will be analyzed and published separately. Absolute concentrations for the most abundant stable intermediates are expected to be within 20% at the current state of development of flame-sampling photoionization mass spectrometry. Results for radicals and minor species (partially based on estimated cross sections) have a probable uncertainty of a factor of 2. This level of accuracy is sufficient for many kinetic modeling purposes.

Ionization energies have been determined for a number of combustion intermediates for the first time. For the linear *i*-C_5H_3 ($H_2CCCCCH$) and *n*-(HCCCHCCH) isomers adiabatic ionization energies of 8.20 ± 0.05 and 8.31 ± 0.05 eV are determined, respectively. For the $CH_2CCHCCH$ isomer an ionization energy of 9.22 ± 0.05 eV was measured, as was an ionization energy of 9.96 ± 0.05 eV for the CH_2CHCH_2CCH isomer.

Acknowledgment. The authors gratefully acknowledge Dr. Paul Winter, Professor Timothy Zwier, and Jaime Stearns for supplying the computer program used to evaluate the Franck−Condon factors and for assistance in its use. The authors are grateful to Paul Fugazzi and Michael Jimenez-Cruz for expert technical assistance. This work is supported by the Division of Chemical Sciences, Geosciences, and Biosciences, the Office of Basic Energy Sciences, the U.S. Department of Energy, in part under Grants DE-FG02-91ER14192 (P.R.W., M.E.L.) and DE-FG02-01ER15180 (T.A.C., J.W.) and by the Chemical Science Division of the U.S. Army Research Office. The work at Argonne is supported under DOE Contract No. W-31-109-ENG-38. T.K. and K.K.-H. are supported by the Deutsche Forschungsgemeinschaft under Contract KO 1363/18-1. Sandia is a multiprogram laboratory operated by Sandia Corporation, a Lockheed Martin Company, for the National Nuclear Security Administration under Contract DE-AC04-94-AL85000. The Advanced Light Source is supported by the Director, Office of Science, Office of Basic Energy Sciences, Materials Sciences Division, of the U.S. Department of Energy under Contract No. DE-AC02-05CH11231 at Lawrence Berkeley National Laboratory. Ford Motor Company is gratefully acknowledged for supplying the propyne used in some of these experiments.

Supporting Information Available: The geometrical structures, harmonic vibrational frequencies, and rotational constants for each of the species. This material is available free of charge via the Internet at http://pubs.acs.org.

References and Notes

(1) Frenklach, M. *Phys. Chem. Chem. Phys.* **2002**, *4*, 2028.
(2) Richter, H.; Howard, J. B. *Phys. Chem. Chem. Phys.* **2002**, *4*, 2038.
(3) Miller, J. A.; Pilling, M. J.; Troe, J. *Proc. Combust. Inst*. **2005**, *30*, 43.
(4) McEnally, C. S.; Pfefferle, L. D.; Atakan, B.; Kohse-Höinghaus, K. *Prog. Energy Combust. Sci.*, in press.
(5) Pope, C. J.; Miller, J. A. *Proc. Combust. Inst.* **2000**, *28*, 1519.
(6) Melius, C. F.; Colvin, M. E.; Marinov, N. M.; Pitz, W. J.; Senkan, S. M. *Proc. Combust. Inst.* **1996**, *26*, 685.
(7) Moskaleva, L. V.; Mebel, A. M.; Lin, M. C. *Proc. Combust. Inst.* **1996**, *26*, 521.
(8) Cool, T. A.; McIlroy, A.; Qi, F.; Westmoreland, P. R.; Poisson, L.; Peterka, D. S.; Ahmed, M. *Rev. Sci. Instrum.* **2005**, *76*, 094102.
(9) Taatjes, C. A.; Hansen, N.; McIlroy, A.; Miller, J. A.; Senosiain, J. P.; Klippenstein, S. J.; Qi, F.; Sheng, L.; Zhang, Y.; Cool, T. A.; Wang, J.; Westmoreland, P. R.; Law, M. E.; Kasper, T.; Kohse-Höinghaus, K. *Science* **2005**, *12*, 1888.
(10) Taatjes, C. A.; Klippenstein, S. J.; Hansen, N.; Miller, J. A.; Cool, T. A.; Wang, J.; Law, M. E.; Westmoreland, P. R. *Phys. Chem. Chem. Phys.* **2005**, *7*, 806.
(11) Hansen, N.; Klippenstein, S. J.; Taatjes, C. A.; Miller, J. A.; Wang, J.; Cool, T. A.; Yang, B.; Yang, R.; Wei, L.; Huang, C.; Wang, J.; Qi, F.; Law, M. E.; Westmoreland, P. R. *J. Phys. Chem. A*, in press.

(12) Berkowitz, J. *Photoabsorption, Photoionization, and Photoelectron Spectroscopy*; Academic Press: New York, 1979.
(13) *Vacuum Ultraviolet Photoionization and Photodissociation of Molecules and Clusters*; Ng, C. Y., Ed.; World Sciences: Singapore, 1991.
(14) Nicholson, A. J. C. *J. Chem. Phys.* **1963**, *39*, 954.
(15) Tanaka, K.; Tanaka, I. *J. Chem. Phys.* **1973**, *59*, 5042.
(16) Miller, J. A.; Klippenstein, S. J. *J. Phys. Chem. A* **2003**, *107*, 7783.
(17) Lamprecht, A.; Atakan, B.; Kohse-Höinghaus, K. *Proc. Combust. Inst.* **2000**, *28*, 1817.
(18) Bittner, J. D. A Molecular Beam Mass Spectrometer Study of Fuel-Rich and Sooting Benzene-Oxygen Flames. PhD Dissertation, Massachusetts Institute of Technology, 1981.
(19) Homann, K. H.; Mochizuki, M.; Wagner, H. G. *Z. Phys. Chem.* **1963**, *37*, 299.
(20) Becke, A. D. *J. Chem. Phys.* **1993**, *98*, 5648.
(21) Hehre, W. J.; Radom, L.; Pople, J. A.; Schleyer, P. v. R. *Ab Initio Molecular Orbital Theory*; Wiley: New York, 1987.
(22) Frisch, M. J.; Trucks, G. W.; Schlegel, H. B.; Scuseria, G. E.; Robb, M. A.; Cheeseman, J. R.; Montgomery, J. A., Jr.; Vreven, T.; Kudin, K. N.; Burant, J. C.; Millam, J. M.; Iyengar, S. S.; Tomasi, J.; Barone, V.; Mnnucci, B.; Cossi, M.; Scalmani, G.; Rega, N.; Petersson, G. A.; Nakatsuji, H.; Hada, M.; Ehara, M.; Toyota, K.; Fukuda, R.; Hasegawa, J.; Ishida, M.; Nakajima, T.; Honda, O.; Kitao, H.; Nakai, H.; Klene, M.; Li, X.; Knox, J. E.; Hratchian, H. P.; Cross, J. B.; Bakken, V.; Adamo, C.; Jaramillo, J.; Gomperts, R.; Stratmann, R. E.; Yazyev, O.; Austin, A. J.; Cammi, R.; Pomelli, C.; Ochterski, J. W.; Ayala, P. Y.; Morokuma, K.; Voth, G. A.; Salvador, P.; Dannenberg, J. J.; Zakrzewski, V. G.; Dapprich, S.; Daniels, A. D.; Strain, M. C.; Farkas, O.; Malick, D. K.; Rabuck, A. D.; Raghavachari, K.; Foresman, J. B.; Ortiz, J. V.; Cui, Q.; Baboul, A. G.; Clifford, S.; Cioslowski, J.; Stefanov, B. B.; Liu, G.; Liashenko, A.; Piskorz, P.; Komaromi, I.; Martin, R. L.; Fox, D. J.; Keith, T.; Al-Laham, M. A.; Peng, C. Y.; Nanayakkara, A.; Challacombe, M.; Gill, P. M. W.; Johnson, B.; Chen, W.; Wong, M. W.; Gonzalez, C.; Pople, J. A. *Gaussian03*; Gaussian Inc., Wallingford, CT, 2004.
(23) Dunning, T. H. *J. Chem. Phys.* **1989**, *90*, 1007.
(24) Amos, R. D.; Bernhardsson, A.; Berning, A.; Celani, P.; Cooper, D. L.; Deegan, M. J. O.; Dobbyn, A. J.; Eckert, F.; Hampel, C.; Hetzer, G.; Knowles, P. J.; Korona, T.; Lindh, R.; Lloyd, A. W.; McNicholas, S. J.; Manby, F. R.; Meyer, W.; Mura, M. E.; Nicklass, A.; Palmieri, P.; Pitzer, R.; Rauhut, G.; Schutz, M.; Schumann, U.; Stoll, H.; Stone, A. J.; Tarroni, R.; Thorsteinsson, T.; Werner, H.-J. *MOLPRO*; a package of ab initio programs designed by H.-J. Werner and P. J. Knowles; 2002.
(25) Lee, T. J.; Rendell, A. P.; Taylor, P. R. *J. Phys. Chem.* **1990**, *94*, 5463.
(26) Doktorov, E. V.; Malkin, I. A.; Man'ko, V. I. *J. Mol. Spectrosc.* **1977**, *64*, 302.
(27) Ruhoff, P. T. *Chem. Phys.* **1994**, *186*, 355.
(28) Ramos, C.; Winter, P. R.; Zwier, T. S.; Pratt, S. T. *J. Chem. Phys.* **2002**, *116*, 4011.
(29) Seburg, R. A.; McMahon, R. J.; Stanton, J. F.; Gauss, J. *J. Am. Chem. Soc.* **1997**, *119*, 10838.
(30) Mebel, A. M.; Lin, S. H.; Yang, X. M.; Lee, Y. T. *J. Phys. Chem. A* **1997**, *101*, 6781.
(31) Woodcock, H. L.; Schaefer, H. F.; Schreiner, P. R. *J. Phys. Chem. A* **2002**, *106*, 11923.
(32) Lossing, F. P.; Traeger, J. C. *J. Am. Chem. Soc.* **1975**, *97*, 1579.
(33) Wang, H.; Brezinsky, K. *J. Phys. Chem. A* **1998**, *102*, 1530.
(34) NIST Standard Reference Database Number 69, J., NIST Chemistry WebBook. http://webbook.nist.gov, Nov 2005.
(35) Catoire, L.; Swihart, M. T.; Gail, S.; Dagaut, P. *Int. J. Chem. Kinet.* **2003**, *35*, 453.
(36) Bieri, G.; Burger, F.; Heilbronner, E.; Maier, J. P. *Helv. Chim. Acta* **1977**, *60*, 2213.
(37) Taatjes, C. A.; Osborn, D. L.; Cool, T. A.; Nakajima, K. *Chem. Phys. Lett.* **2004**, *394*, 19.
(38) Kamphus, M.; Liu, N. N.; Atakan, B.; Qi, F.; McIlroy, A. *Proc. Combust. Inst.* **2003**, *29*, 2627.
(39) Cool, T. A.; Nakajima, K.; Mostefaoui, T. A.; Qi, F.; McIlroy, A.; Westmoreland, P. R.; Law, M. E.; Poisson, L.; Peterka, D. S.; Ahmed, M. *J. Chem. Phys.* **2003**, *119*, 8356.
(40) Maier, J. P. *Angew. Chem., Int. Ed. Engl.* **1981**, *20*, 638.
(41) Hansen, N.; Miller, J. A.; Taatjes, C. A.; Wang, J.; Cool, T. A.; Law, M. E.; Westmoreland, P. R. *Proc. Combust. Inst.*, submitted for publication, 2005.
(42) Qi, F. University of Science at Technology of China, Hefei, China. Personal communication, 2005.
(43) Lossing, F. P.; Holmes, J. L. *J. Am. Chem. Soc.* **1984**, *106*, 6917.
(44) Derrick, P. J.; Asbrink, L.; Edqvist, O.; Jonsson, B. O.; Lindholm, E. *Int. J. Mass Spectrom. Ion Phys.* **1971**, *6*, 203.
(45) Carlier, P.; Mouvier, G.; Mesnard, D.; Miginiac, L. *J. Electron. Spectrosc. Relat. Phenom.* **1979**, *16*, 147.
(46) Masclet, P.; Mouvier, G.; Bocquet, J. F. *J. Chim. Phys. Phys.—Chim. Biol.* **1981**, *78*, 99.
(47) Cool, T. A.; Wang, J.; Hansen, N.; Westmoreland, P. R. Unpublished data, 2005.
(48) Delfau, J. L.; Vovelle, C. *J. Chim. Phys. Phys.—Chim. Biol.* **1985**, *82*, 747.
(49) Westmoreland, P. R. Experimental and Theoretical Analysis of Oxidation and Growth Chemistry in a Fuel-Rich Acetylene Flame. PhD Dissertation, Massachusetts Institute of Technology, 1986.
(50) Westmoreland, P. R.; Howard, J. B.; Longwell, J. P. *Proc. Combust. Inst.* **1986**, *21*, 773.
(51) Miller, J. A.; Melius, C. F. *Combust. Flame* **1992**, *91*, 21.
(52) Melius, C. F.; Miller, J. A.; Evleth, E. M. *Proc. Combust. Inst.* **1992**, *24*, 621.
(53) Bittner, J. D.; Howard, J. B. *Proc. Combust. Inst.* **1982**, *19*, 211.
(54) Smith, R. D. *Combust. Flame* **1979**, *35*, 179.
(55) Atakan, B.; Lamprecht, A.; Kohse-Höinghaus, K. *Combust. Flame* **2003**, *133*, 431.
(56) Alatorre, G. G.; Böhm, H.; Atakan, B.; Kohse-Höinghaus, K. *Z. Phys. Chem.* **2001**, *215*, 981.
(57) Homann, K. H.; Wagner, H. G. *Ber. Bunsen-Ges. Phys. Chem.* **1965**, *69*, 20.
(58) Moskaleva, L. V.; Lin, M. C. *J. Comput. Chem.* **2000**, *21*, 415.
(59) Knyazev, V. D.; Slagle, I. R. *J. Phys. Chem. A* **2002**, *106*, 5613.
(60) Cool, T. A.; Nakajima, K.; Taatjes, C. A.; McIlroy, A.; Westmoreland, P. R.; Law, M. E.; Morel, A. *Proc. Combust. Inst.* **2005**, *30*, 1681.
(61) Nguyen, T. L.; Le, T. N.; Mebel, A. M. *J. Phys. Org. Chem.* **2001**, *14*, 131.
(62) Bieri, G.; Dill, J. D.; Heilbronner, E.; Maier, J. P.; Ripoll, J. L. *Helv. Chim. Acta* **1977**, *60*, 629.
(63) Roy, K.; Braun-Unkhoff, M.; Frank, P.; Just, T. *Int. J. Chem. Kinet.* **2001**, *33*, 821.
(64) Burcat, A.; McBride, B. *Ideal Gas Thermodynamics Data for Combustion and Air Pollution Use*; Technion Aerospace Eng. Rep. 697, Haifa, Israel: Technion Department of Aerospace Engineering, Dec 1993.
(65) Bacskay, G. B.; Martoprawiro, M.; Mackie, J. C. *Chem. Phys. Lett.* **1998**, *290*, 391.
(66) Allinger, N. L.; Dodziuk, H.; Rogers, D. W.; Naik, S. N. *Tetrahedron* **1982**, *38*, 1593.
(67) Fraser, F. M.; Prosen, E. J. *J. Res. Natl. Bur. Stand. (U.S.)* **1955**, *54*, 143.